Thermal Plasma-processed Natural Hydroxyapatite-MnO₂ Nanoparticles as a Reusable and Green Heterogeneous Catalyst for Aerobic Oxidation of Benzylic Alkyl Arenes and Alcohols

A. Shaabani[a,*], M.S. Laeini[b], S. Mohsenian[c], B. Shokri[c,d] and R. Afshari[b]

[a]*Faculty of Chemistry, Shahid Beheshti University*
[b]*Faculty of Chemistry, Shahid Beheshti University, G. C., Evin, Tehran 19396-4716, Tehran, Iran*
[c]*Laser-Plasma Research Institute, Shahid Beheshti University, G.C., Evin, Tehran 19839-63113, Iran*
[d]*Physics Department, Shahid Beheshti University, G.C., Evin, Tehran 19839-63113, Iran*

(Received 16 October 2017, Accepted 20 November 2017)

In the present work, we have reported the *in situ* oxidation of manganese(II) acetate to MnO₂ nanoparticles through the thermal plasma carbonized natural hydroxyapatite (MnO₂/TP-NHAp) as a neoteric sustainable method. Interestingly, the thermal plasma-processed surface of the NHAp shows a great ability for oxidation of the manganese(II) without need of any external oxidizing agents. The catalyst was characterized by X-ray diffraction (XRD), Brunauer-Emmett-Teller (BET), thermogravimetric analysis (TGA), flame atomic absorption spectroscopy (FAAS), Fourier transform infrared (FT-IR), scanning electronic microscopy (SEM) and energy dispersive spectroscopy (EDS). The catalytic activity of MnO₂/TP-NHAp was investigated in the selective aerobic oxidation of alcohols and benzylic alkyl arenes at 80 °C in toluene under an atmospheric pressure of air as a source of oxidant. Since the catalyst can be easily recovered and reused at least for four consecutive cycles without losing significant activity and selectivity, it showed admirable potential in reusable catalysis.

Keywords: Natural hydroxyapatite, Thermal plasma-processed, Heterogeneous catalyst, Aerobic oxidation, MnO₂ nanoparticle

INTRODUCTION

In recent years, development of heterogeneous catalyst systems has become a more challenging task that has encouraged chemists to design cost effective, inexpensive and eco-friendly catalytic processes [1-3]. Compared to homogeneous catalytic systems which suffer from some difficulties such as tedious work-up procedures, utilizing of hazardous terminal oxidants, and generating considerable amount of toxic wastes [4], supported heterogeneous catalysts have been received widespread attentions for large-scale oxidation operations. Obviously, in this scope, it would be far better to introduce an environmentally friendly, non-toxic and green supported heterogeneous catalytic system [5,6].

Hydroxyapatite (HAp, $Ca_{10}(PO4)_6(OH)_2$) is a crystal form of calcium phosphate with either monoclinic or hexagonal crystal symmetry [7] that is commonly one of the major constituents of the inorganic component in bone tissue and teeth. This bio-mineral possesses excellent properties with unique structure and complex forms which are of great interest for the fertilizer industries [8], drug delivery [9], protein chromatography applications, [10] heterogeneous catalysis systems, [11] and so forth. In addition, this compound has shown a high chemical and thermal stability and has a structural flexibility. Consequently, extensive studies have been performed in the area of synthesis of heterogeneous catalysts based on hydroxyapatite (HAp-supported transition metals), such as gold [12], ruthenium [13,14], palladium [15] and copper [16]. The accessibility of hydroxyapatite for supporting transition metals is commonly attributed to its high ion-exchange, adsorption ability and also presence of both acidic and basic sites with adequate strength in a single crystal lattice [17,18], as a result, it can be utilized for a wide range of catalytic reactions [19-21]. These properties of hydroxyapatite prompted us to focus on the utilization of natural hydroxyapatite for the stabilization of metal oxide

---

*Corresponding author. E-mail: a-shaabani@sbu.ac.ir

nanoparticles. Among the various transition metal oxides, manganese dioxide has received appreciable attention due to its accessibility, economics, outstanding physical and chemical properties under ambient conditions and importantly excellent catalytic performance [22,23]. Manganese dioxide has been widely used as an effective oxidizing agent and is crucial for various types of organic transformations, for example, hydration of nitriles [24], alkylation [25] and coupling reactions [26]. Interestingly, in the area of oxidation reactions, supported manganese dioxide has increasingly been applied and particularly tested for the aerobic oxidation reactions [27-29].

Until now, research efforts have been made to prepare MnO_2 nanoparticles through different procedures, employing Mn(II) salt with an oxidizing reagent such as $(NH_4)_2S_2O_8$, $KMnO_4$ and H_2O_2 [30-33]. With no doubt, some of the oxidizing reagents such as $KMnO_4$ not only can cause surface and chemical changes on support [34], but also they might leave a large amount of residual material. As a result, it would be worthwhile to introduce a unique method for the syntheses of MnO_2 nanoparticles, which have no destructive effect on the surface of catalyst with an eco-compatible feature.

Herein, we report the *in situ* oxidizing of manganese(II) acetate to MnO_2 by thermal plasma carbonized natural hydroxyapatite as a bio-support. It should be noted here that in our previous report, the $KMnO_4$ was reduced to MnO_2 nanoparticles by the surface of natural hydroxyapatite [35]. However, in the present work, the thermal plasma processed surface of natural hydroxyapatite exhibits a different chemical behavior and acts as an oxidizing support for oxidation of Mn(II) to MnO_2 nanoparticles. To the best of our knowledge, this is the first report for the *in situ* transformation of Mn(II) to MnO_2 nanoparticles without the utilization of any toxic oxidizing additive or harsh reaction conditions. Furthermore, the catalytic activities of synthesized composite toward the aerobic oxidation of arenes and alcohols have been investigated (Scheme 1).

EXPERIMENTAL

All chemicals were purchased from Aldrich or Merck companies and used without further purification. IR spectra were recorded on a Bomem MB-Series FT-IR

spectrophotometer. Mn(IV) determination was carried out on an FAAS (Shimadzu model AA-680 flame atomic absorption spectrometer). Thermogravimetric analysis (TGA) was carried out using an STA 1500 instrument at a heating rate of 10 °C min^{-1} in air. Ultrasonic bath (EUROSONIC®4D ultrasound cleaner with a frequency of 50 kHz and an output power of 350 W) was used to disperse materials in solvent. The textural structures were measured by N_2 adsorption at 196 °C in a micromeritics TriStar ASAP 3000 system, and specific surface areas of the as-prepared samples were measured using Brunauer-Emmett-Teller (BET). X-ray powder diffraction (XRD) data were collected by a XD-3A diffractometer using Kα radiation. Scanning electron microscopy (SEM) and EDX observations were carried out by an electron microscopy Philips XL-30 ESEM. All samples were sputtered with gold before observation.

Synthesis of Thermal Plasma-processed Natural Hydroxyapatite Nanocomposite (TP-NHAp)

NHAp was synthesized according to our previously reported method [36]. To obtain thermal plasma processed natural hydroxyapatite nanoparticles (TP-NHAp), thermal plasma procedure for carbonization of organic compounds, such as collagen, was utilized. The heat source of the carbonizer is a DC plasma arc torch that produces a very high temperature plasma gas (up to 10000 °C). Plasma carbonization is a thermal pyrolytic reaction which converts the organic materials to carbon or a carbon-containing residue. The most favorable experimental condition for the required pyrolytic reaction is to produce extremely high temperatures in an atmospheric pressure oxygen-starved environment. In this case, initially the vacuum chamber was evacuated down to residual air pressure 30 mTorr by means of a rotary pump. The chamber was then filled with argon (with purity of 99.99%) as an ambient gas up to the required operating working pressure in the range of 1-2 atm. In the highly thermal plasma zone, there is a large fraction of reactive and high energetic species such as electrons, ions and excited molecules together with the high energy radiation. When bone is injected into plasma, it is heated very rapidly by the plasma and further chemical reactions occur. In these experiments the carbonization processing was performed at adjustable electrical conditions with the electrical plasma column current of 100-150 A.
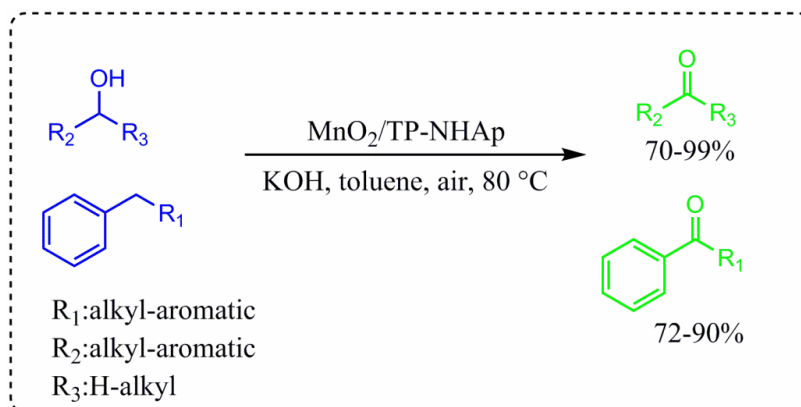
Scheme 1. Oxidation of alcohols and benzylic alkyl arenes using MnO$_2$/TP-NHAp
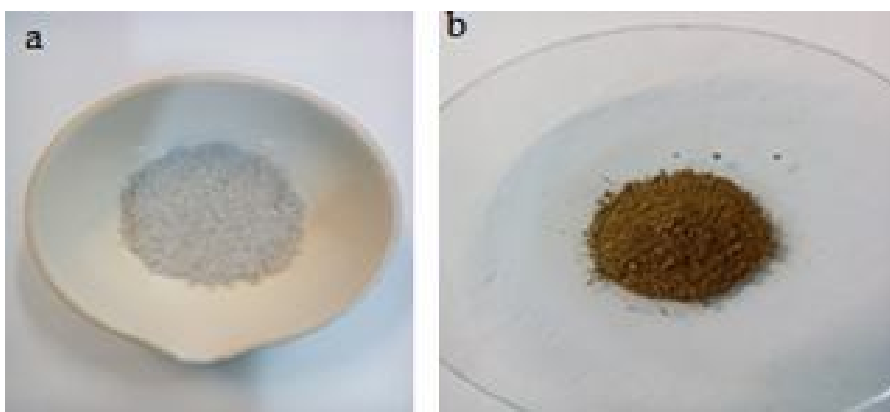
**Fig. 1.** Digital images of a: TP-NHAp and b: MnO$_2$/TP-NHAp.

Furthermore, the plasma treatment of the bone lasted approximately 3-15 min [37].

Synthesis of MnO$_2$/TP-NHAp

TP-NHAp (1.00 g) and aqueous solution of Mn(OAc)$_2$ (0.50 g. in 10 ml of deionized water) were mixed and placed in an ultrasonic bath (50 KHz) for 20 min for dispersing the metal ions in the surface of carbonized hydroxyapatite. After stirring at room temperature for 24 h, the brown catalyst (Fig. 1) was filtered and washed with water (3 × 10 ml) and ethanol (3 × 10 ml), then dried under vacuum at 100 °C for 8 h.

General Procedure for the Catalytic Aerobic Oxidation of Organic Compounds by MnO$_2$/TP-NHAp

In a general reaction, a mixture of organic compound (1.00 mmol), MnO$_2$/TP-NHAp (5.30 mol% MnO$_2$, 0.10 g) and KOH (0.50 mmol) was added to a two-necked flask containing toluene (4.00 ml) as solvent under bubbling of air (25 ml min^{-1}) at 80 °C under reflux conditions. The progress of the reaction was followed by gas chromatography (GC). After completion of the reaction, the mixture was filtered and analysis of the crude product was done using GC. GC yields were obtained using n-decane as
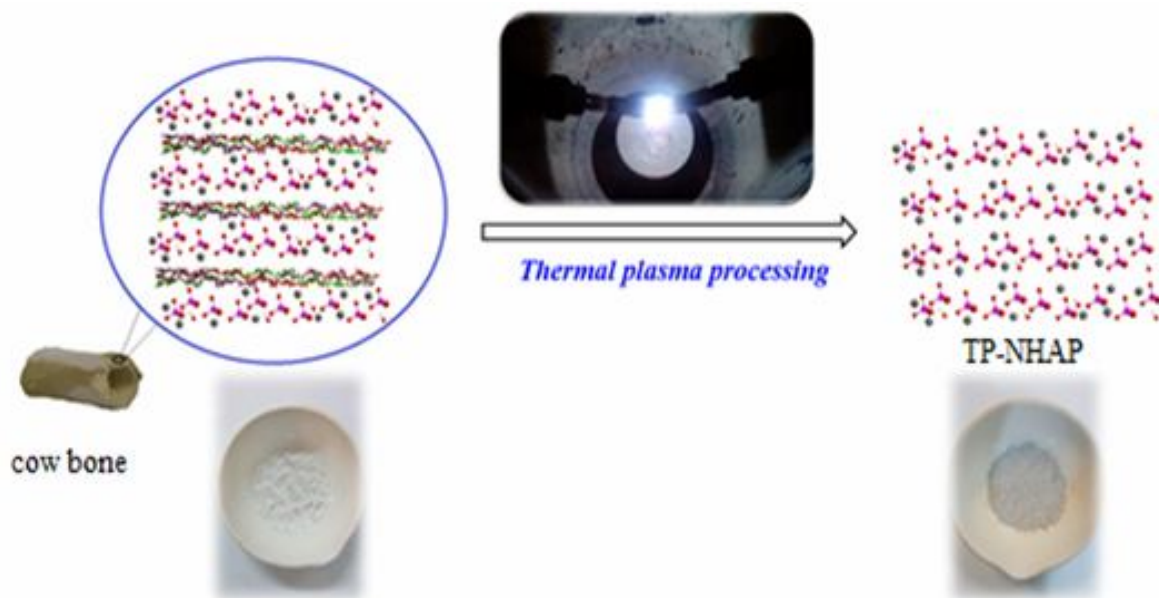
Scheme 2. Synthesis of MnO$_2$ NPs through thermal plasma-processed natural hydroxyapatite nanocomposite (MnO$_2$/TP-NHAp).
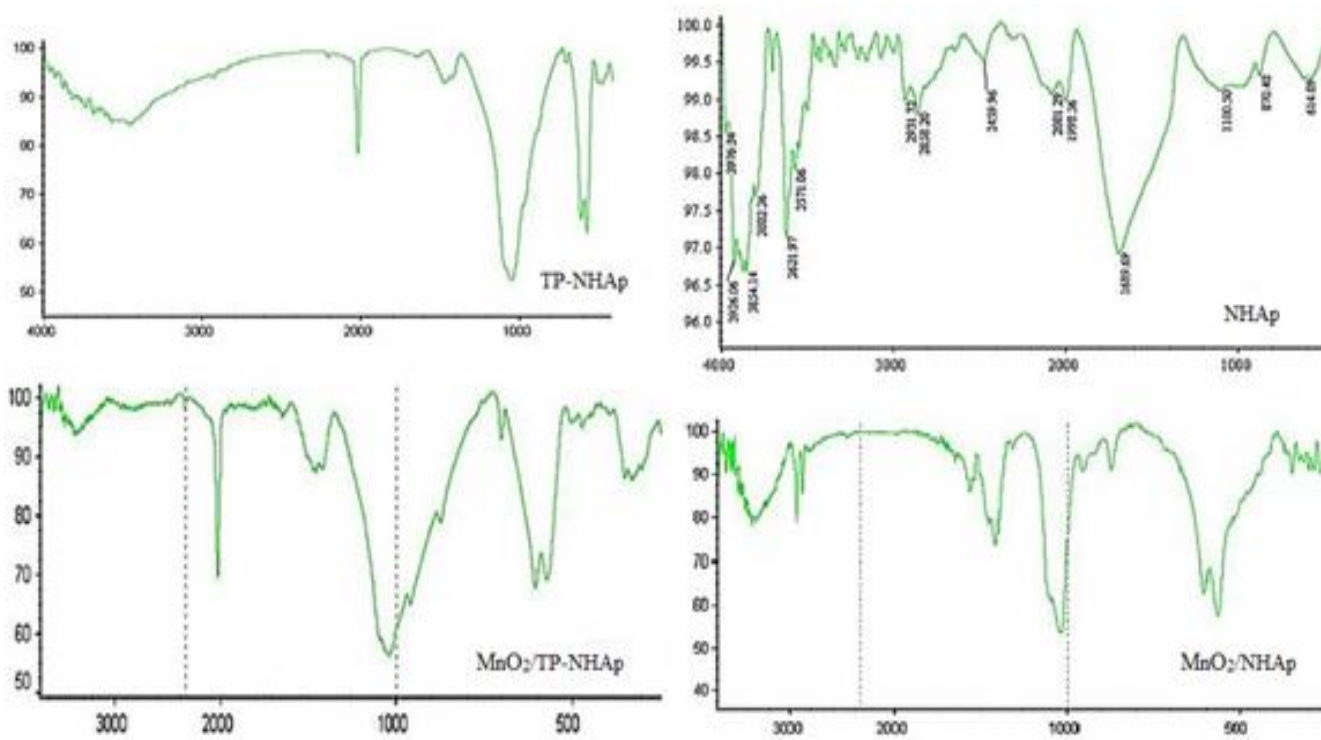

Fig. 2. FT-IR spectra of synthesized composites.

an internal standard based on the amount of organic compound employed relative to authentic standard product.

Gram-Scale Reaction

Diphenylmethanol (10.00 mmol, 1.84 g) was added to a two-necked flask fitted with mixture of MnO$_2$/TP-NHAp (1.00 g) and KOH (5.00 mmol) in 40 ml of toluene. The mixture was heated at 80 °C for 3 h with continuous bubbling of air with a flow rate of 25 ml min^{-1} under reflux conditions. Upon completion, the mixture was cooled to room temperature and the catalyst was separated by filtration and the solvent was evaporated. Benzophenone (m.p.: 49-51 °C) as a main product was isolated in 97% yield (1.77 g).

RESULTS AND DISCUSSION

Plasma carbonization is a thermal pyrolytic reaction that converts the organic materials to carbon or a carbon-containing residue in extremely high temperatures in an atmospheric pressure oxygen-starved environment [38]. The thermal plasma processed-natural hydroxyapatite nanoparticles (TP-NHAp) were synthesized based on the procedure which used for the thermal plasma carbonization of organic compounds (Scheme 2). The injected bone was heated very rapidly by the plasma and further chemical reactions occur. In this experiment, the carbonization process was performed at adjustable electrical conditions with the electrical plasma column current of 100-150 A. The plasma treatment of the bone lasted approximately 3-15 min [33]. Subsequently, the MnO$_2$ particles were synthesized on the surface of TP-NHAp and the MnO$_2$ content was determined as 5.30 mol% using FAAS. Interestingly, the thermal plasma modified natural hydroxyapatite nanocomposite shows a great ability for oxidizing the Mn(II) salts to MnO$_2$ without need of any external agent unlike to the pure natural hydroxyapatite which shows the reducing behavior as demonstrated in our previous work [35].

FT-IR spectra of TP-NHAp and MnO$_2$/TP-NHAp in comparison with NHAp and MnO$_2$/NHAp are shown in Fig. 2. The spectrum of MnO$_2$/TP-NHAp shows a peak at 780 cm^{-1} due to the vibration mode of the P-O bond. The strong stretching band at 1070 cm^{-1} is attributed to the P-O

vibrations. The peak at 2010 cm^{-1} is related to the overtone band of PO$_4^{3-}$ ions. Interestingly, before using thermal plasma-processed this strong band was not observed. The broad band at 3400 cm^{-1} is due to the stretching vibration of the lattice OH$^-$ ions [39]. In addition, the absorption band at about 550 cm^{-1} in the spectrum of MnO$_2$/TP-NHAp is attributed to the vibration of (Mn-O) bonds [40].

All samples were characterized by powder X-ray diffraction (PXRD). XRD phase analyses of TP-NHAp and MnO$_2$/TP-NHAp have been shown in Fig. 3. In the XRD pattern of NHAp the weak peak at 2θ = 25.8° and a sharp peak at 32° is attributed to Hap [41].The strong and sharp peak at 2θ = 29.8^o and a week peak at 2θ = 32.10^o are attributed to TP-NHAp. Two sharp peaks at 25.84^o and 39.22^o, and two weak peaks at 34.04^o and 64.23^o from the MnO$_2$/TP-NHAp spectra can be attributed to the MnO$_2$ [29].

Brunauer-Emmett-Teller (BET) method was used to estimate the specific surface area of the NHAp and TP-NHAp (Table 1). BET calculations based on N$_2$ adsorbed at P/P0 ≈ 0.99 indicated the specific surface area and increase the pore volume of TP-NHAp. It could be concluded from the results that the organic materials inside of the bone were decomposed during the thermal plasma treated.

The SEM analyses have been used to study the structure and morphology of the thermal plasma-processed hydroxyapatite and MnO$_2$ nanoparticles-carbonized hydroxyapatite nanocomposite (Fig. 4). The SEM images of MnO$_2$/TP-NHAp confirmed that after immobilization of Mn nanoparticles the final product is composite (Figs. 4c, d). In addition, the chemical composition of the MnO$_2$/TP-NHAp was investigated using energy dispersive spectroscopy (EDS) which proves the presence of P, Ca, Mn and O in the structure of MnO$_2$/TP-NHAp nanohybrid (Fig. 4e).

The thermal stability of the synthesized catalyst was investigated by TGA analysis. As indicated from Fig. 5, TP-NHAp is highly stable and only show an initial weight loss (3 wt. %) due to the absorbed water around 100 °C. Also, the curves showed that TP-NHAp is more stable than NHAp. For MnO$_2$/TP-NHAp the curve confirmed that MnO$_2$ spontaneously deposited on the TP-NHAp, the weight loss between 200-400 °C corresponds to the loss of lattice oxygen atoms [46]. The MnO$_2$/TP-NHAp catalyst exhibits good thermal stability even at 800 °C.

To demonstrate the catalytic activity of the synthesized
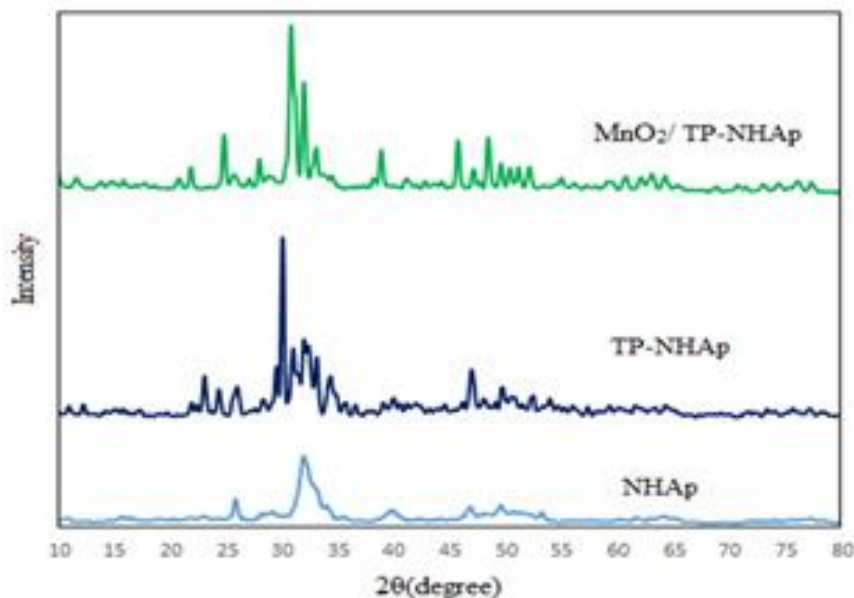
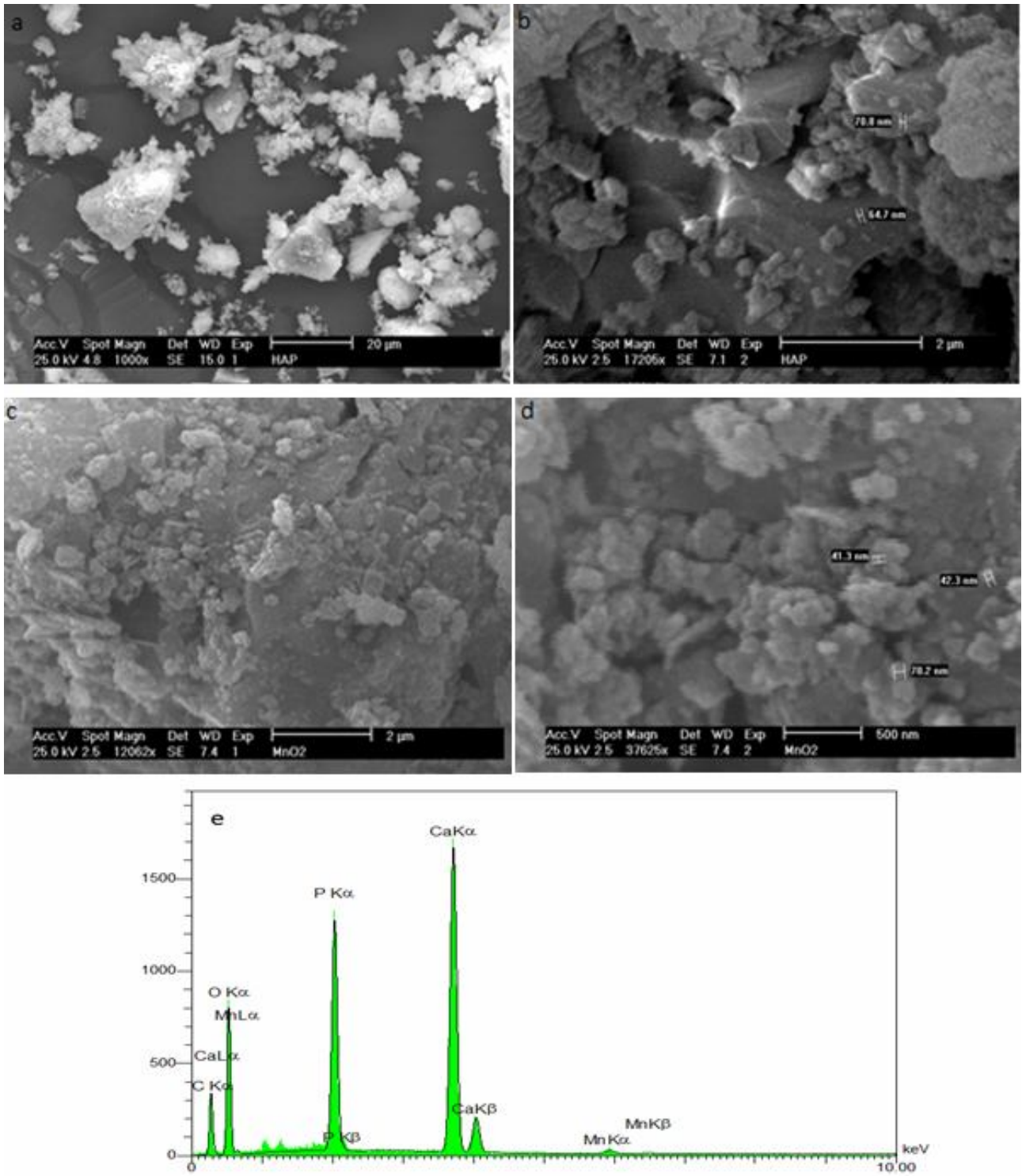**Fig. 3.** XRD patterns of NHAp, TP-NHAp and MnO$_2$/TP-NHAp.

Table 1. Textural Properties of the Prepared Materials Determined from Nitrogen Physisorption

Entry	Material	S_{BET} $(m^2\ g^{-1})^a$	V_p $(cm^3\ g^{-1})^b$	D_{BJH} $(nm)^c$
1	Bone	1.6405	0.0393	53.04
2	TP-NHAp	21.438	0.0906	6.06

$^a S_{BET}$: Specific surface area. ^{b}Pore volume. $^c D_{BJH}$: Average pore size diameter.

MnO$_2$/TP-NHAp, oxidation of alcohols and benzylic alkyl arenes to their corresponding carbonyl compounds were examined. For this purpose, the aerobic oxidation of 1-phenylethanol in toluene at 80 °C as a model reaction was performed. Under the reaction conditions, the selectivity of reaction for the formation of corresponding ketone was 100%, although the conversion was low (Table 2, Entries 1-4). In continuation, a variety of organic and inorganic common bases were applied for the oxidation process. When the oxidation reaction was carried out in the presence of K$_2$CO$_3$ as available and safe base, the yield was perfectly reasonable, whereas the reaction time was slightly prolonged (Table 2, Entry 5). As seen in Table 2, KOH showed the best results with high yields (Entry 6). In addition, several experiments were performed for the solvent optimization. 1-Phenylethanol oxidation was performed in various solvents such as toluene, n-hexane, CH$_3$CN, H$_2$O, EtOAc and EtOH. The reaction carried out in CH$_3$CN and n-hexane in the long reaction times in order to produce reasonable yields (52-56%) (Table 3, Entries 1-4). The reaction was completely stopped in H$_2$O and EtOH (Table 3, Entries 6,7). As indicated in Table 3, the MnO$_2$/TP-NHAp showed the best catalytic activity in the toluene in terms of yield and time (Table 3, Entry 1). Also,

Fig. 4. SEM images of the synthesized hydroxyapatite (a,b), MnO₂/TP-NHAp (c,d) and EDS analysis of MnO₂/TP-NHAp (e)
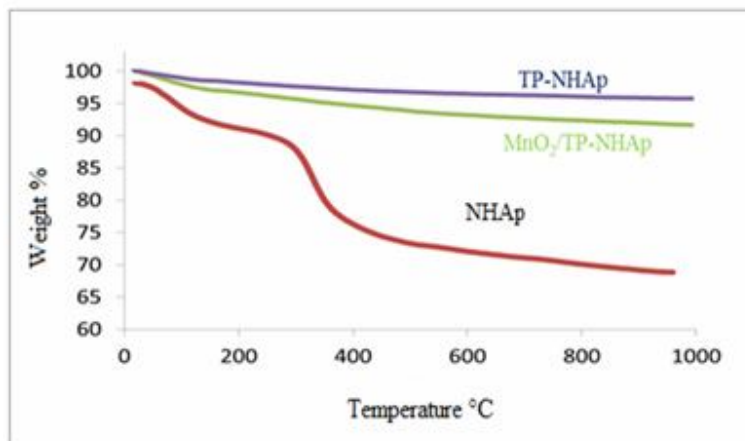
Fig. 5. TGA curves of NHAp, TP-NHAp and MnO$_2$/TP-NHAp.

Table 2. Optimization of Reaction Conditions for Aerobic Oxidation Reactions

Entry	Catalyst	Amount of catalyst (mol%)	Time (h)	Base	Conv. (%)	Yield (%)
1	MnO$_2$/TP-NHAp	0.03 g (1.00)	8	-	12	12
2	MnO$_2$/TP-NHAp	0.05 g (3.00)	8	-	17	17
3	MnO$_2$/TP-NHAp	0.10 g (6.00)	8	-	26	26
4	MnO$_2$/TP-NHAp	0.15 g (9.00)	8	-	28	28
5	MnO$_2$/TP-NHAp	0.10 g (6.00)	8	K$_2$CO$_3$	79	79
6	MnO$_2$/TP-NHAp	0.10 g (6.00)	2.30	KOH	93	93
7	MnO$_2$/TP-NHAp	0.10 g (6.00)	3	NaOH	84	84
8	MnO$_2$/TP-NHAp	0.10 g (6.00)	4	Et$_3$N	72	72
9	MnO$_2$/TP-NHAp	0.10 g (6.00)	4	t-BuOK	75	75

Reaction conditions: 1-phenylethanol (1.00 mmol), toluene (4 ml), base (0.5 mmol) 80 °C and air as oxidant.
[a]Conversion and yield determined by GC analysis.

the effect of temperature was investigated and the optimal reaction temperature was 80 °C. Therefore, the reaction of 1-phenylethanol with MnO$_2$/TP-NHAp (5.30% mol) in the presence of KOH (0.50 mol%) in toluene as a solvent at 80 °C gave the optimum yield of the product.

In order to extend the scope of the reaction, we performed the oxidation of various alcohols under optimized reaction conditions. As shown in Table 4, this method was successfully applied for the transformation of both primary and secondary alcohol derivatives. Primary alcohols are converted into the corresponding aldehydes in good yields (Table 4, Entries 1-5). Furthermore, it was

Table 3. Comparative Study between Various Solvents

Entry	Solvent	Temperature (°C)	Time (h)	Con. (%)	Yield (%)
1	Toluene	80	2.30	93	93
2	Toluene	100	2.30	94	94
3	n-Hexane	60	5	56	56
4	CH$_3$CN	80	5	52	52
5	EtOAc	70	5	30	30
6	H$_2$O	100	8	0	0
7	EtOH	75	8	0	0

Reaction conditions: 1-phenylethanol (1 mmol), MnO$_2$/TP-NHAp (0.10 g, 6 mol%), KOH (0.50 mmol), air.

Table 4. Aerobic Oxidation of Alcohols with MnO$_2$/TP-NHAp as a Catalyst[a]
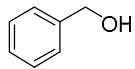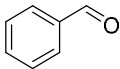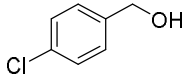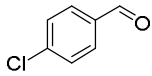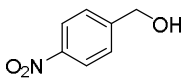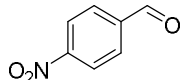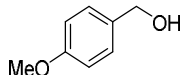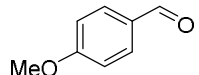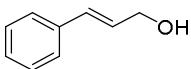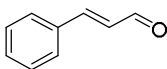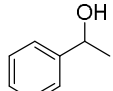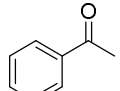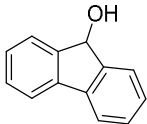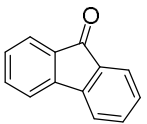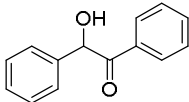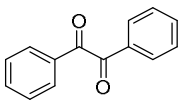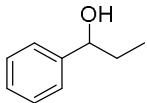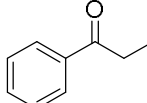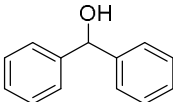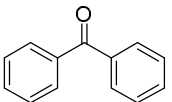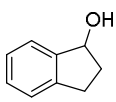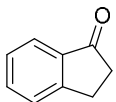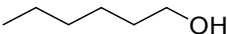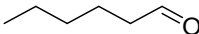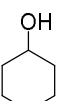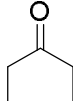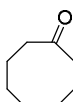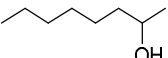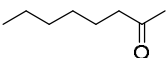
Entry	Alcohol	Product	Time (h)	Yield (%)[b]	Selectivity (%)[b]
1			1	99	99
2			1.30	90	99
3			1.30	92	99
4			1	82	99
5			3	70	98
6			2.30	93	99

Table 4. Continued

7			3	90	99
8			3	89	99
9			4	85	99
10			3	97	99
11			3	90	99
12			7	72	99
13			7	76	99
14			7	75	99
15			7	71	99

[a]Reaction conditions: alcohol (1.00 mmol), MnO$_2$/TP-NHAp (0.10 g, 6.00 mol%), KOH (0.5 mmol), toluene (4 ml), air oxidant, 80 °C. [b]Yield and selectivity determined by GC analysis.

observed that aldehydes did not undergo subsequent oxidation to carboxylic acids. Similarly, ketones were achieved in comparable yields from the oxidation of secondary alcohols (Table 4, Entries 6-11). Among the different range of alcohols, the oxidation of aliphatic alcohols to the corresponding aliphatic carbonyl compounds still remains a major challenge for both homogeneous and heterogeneous catalysts reported so far, owing to their low

reactivity [42]. As shown in Table 4, the reasonable yields of aliphatic alcohols are achieved in this report (Table 4, Entries 12-15).

Furthermore, the capability of this catalyst was evaluated in the aerobic oxidation of benzylic alkyl arenes to related carbonyl compounds in the same optimizing reaction condition. The results are summarized in Table 5.

After detecting that thermal plasma-processed surface of

Table 5. Aerobic Oxidation of Benzylic Alkyl Arenes with MnO$_2$/TP-NHAp as a Catalyst[a]

$$\text{Ar} \diagdown \text{R} \xrightarrow[\text{toluene, air, 80 °C}]{\text{MnO}_2/\text{TP-NHAp (6 mol\%), KOH}} \text{Ar} \diagup \overset{\text{O}}{\diagdown} \text{R}$$
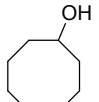
Entry	Alcohol	Product	Time (h)	Yield (%)	Selectivity (%)
1			10	90	99
2			12	88	99
3			12	80	98
4			12	86	99
5			13	72	99

[a]Reaction conditions: benzylic alkyl arenes (1.00 mmol), MnO$_2$/TP-NHAp (0.100 g, 6.00 mol%), KOH (0.5 mmol), toluene (4 ml), air oxidant, 80 °C. [b]Yield and selectivity determined by GC analysis.

the natural hydroxyapatite has the ability to oxidize the manganese(II), we decided to examine the catalytic activity of the TP-NHAp without MnO$_2$ nanoparticles for aerobic oxidation of benzyl alcohol. As indicated in Table 6, when 0.10 g of transition metal-free TP-NHAp nanoparticles is used, the reaction is performed in a good yield (Entry 2). In addition, natural hydroxyapatite nanoparticles were heated by classical heating oven at 1000 °C for 2 h and used for oxidation processes under the same conditions (CH-NHAp). The results show that the reaction has been performed in lower yield (Table 6, Entry 3). Moreover, it should be noted here that the bone before applying thermal plasma carbonization seems to be catalytically inactive for aerobic oxidation reaction, as indicated by a very low yield of 15%

for benzyl alcohol at 110 °C (Table 6, Entry 4). Finally, in one control of experiment without catalyst which was conducted at 110 °C, a low value of the product was detected by GC method (Table 6, Entry 5).

It can be concluded from the results that metal-free TP-NHAp also has the great ability for oxidation of the organic compounds. Although, in comparison with MnO$_2$/TP-NHAp, the conditions such as temperature and the time of the reaction are more violent.

In light on the gram-scale capability of the procedure, the cost-effective gram scale oxidation of diphenylmethanol at 80 °C for 3 h with continuous bubbling of air with a flow rate of 25 ml min^{-1} were developed. Benzophenone as a main product was isolated in 97% yield which confirmed

Table 6. Comparison of the Catalytic Activities for Aerobic Oxidation of Benzyl Alcohol[a]

Entry	Catalyst	Amount of catalyst (g)	Time (h)	Temperature (°C)	Yield (%)[b]
1	MnO_2/TP-NHAp	0.10	1	80	99
2	TP-NHAp	0.10	5	110	85
3	CH-NHAp	0.10	6	110	38
4	Bone	0.10	6	110	15
5	-	-	5	110	13

[a]Reaction conditions: benzyl alcohol (1.00 mmol), toluene (4.0 ml), KOH (0.50 g), air (1.0 atm).   [b]Yield determined by GC analysis.

	1	2	3	4
Yield %	93	92	90	88
Selectivity %	99	99	98	97
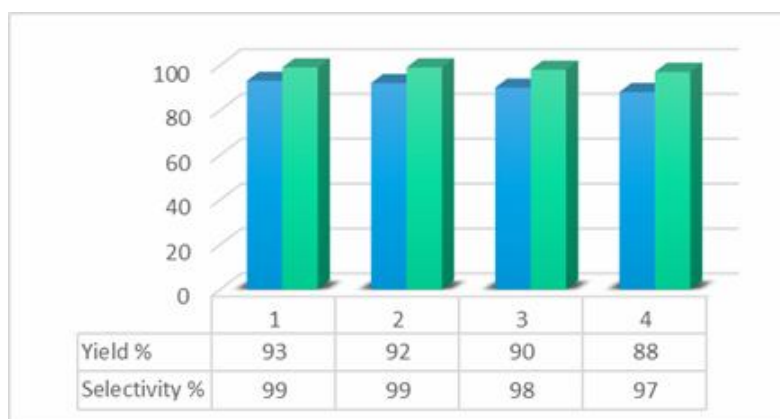
Fig. 6. Reuseability of the MnO_2/TP-NHAp catalyst for oxidation reaction.

the great gram-scale capability of the MnO_2/TP-NHAp catalytic procedure. Subsequently, the reusability of the MnO_2/TP-NHAp was examined for the oxidation reaction of 1-phenylethanol. The catalyst was reused in the reaction after washing with acetone and drying under vacuum at 60 °C. This procedure was performed for four consecutive cycles. The results demonstrated that only minor decreases in the reaction yields were observed and the recovered catalyst retained a significant fraction of the original activity and selectivity.

CONCLUSIONS

In this paper, an efficient and environmentally benign route for the synthesis of MnO_2 nanoparticles on the surface of thermal plasma-processed natural hydroxyapatite has been described. MnO_2/TP-NHAp as a bio-supported heterogeneous catalytic system was prepared from *in situ* oxidation of Mn(II) on the surface of plasma-treated natural hydroxyapatite without need of any oxidizing reagent. The result of this significant accomplishment confirmed the selective aerobic oxidation of various primary, secondary aliphatic and aromatic alcohols and benzylic alkyl arenes into their corresponding carbonyl compounds with good to excellent yields. Also, the catalyst has good chemical stability in the reaction media, proved by investigating the recyclability of the catalyst. In addition, catalyst was successfully recovered from the reaction mixture and reused

for four subsequent reaction cycles without any remarkable decrease in its catalytic activity and selectivity. Meanwhile, the catalytic system could be a great candidate for large scale oxidation transformations. Therefore it seemed that MnO$_2$/TP-NHAp catalyst can shift from a laboratory to industrial productions. Efforts are currently underway to improve the better performance of TP-NHAp as an innovative metal-free bio-support for oxidation process.

ACKNOWLEDGEMENTS

REFERENCES

[1]   T. Mallat, A. Baiker, Chem. Rev. 104 (2004) 3037.

[2]   T. Punniyamurthy, S. Velusamy, J. Iqbal, Chem. Rev. 105 (2005) 2329.

[3]   S.E. Allen, R.R. Walvoord, R. Padilla-Salinas, M.C. Kozlowski, Chem. Rev. 113 (2013) 6234.

[4]   S. Weinreb, B. Trost, I. Fleming, Comprehensive Organic Synthesis. In: B.M. Trost, I. Fleming (Eds.), 1991, p. 5.

[5]   E. Doustkhah, S. Rostamnia, B. Gholipour, B. Zeynizadeh, A. Baghban, R. Luque, Mol. Catal. 434 (2017) 7.

[6]   S. Rostamnia, E. Doustkhah, Z. Karimi, S. Amini, R. Luque, Chem. Cat. Chem. 7 (2015) 1678.

[7]   D. Haverty, S.A. Tofail, K.T. Stanton, J.B. McMonagle, Phys. Rev. B 71 (2005) 094103.

[8]   N. Kottegoda, I. Munaweera, N. Madusanka, V. Karunaratne, Curr. Sci. (2011) 73.

[9]   H. Yang, L. Hao, N. Zhao, C. Du, Y. Wang, Cryst. Eng. Comm. 15 (2013) 5760.

[10]   M.J. Gorbunoff, Methods Enzymol. 117 (1985) 370.

[11]   K. Mori, K. Yamaguchi, T. Hara, T. Mizugaki, K. Ebitani, K. Kaneda, J. Am. Chem. Soc. 124 (2002) 11572.

[12]   Y. Liu, H. Tsunoyama, T. Akita, S. Xie, T. Tsukuda, ACS Catal. 1 (2010) 2.

[13]   H. Durak, M. Gulcan, M. Zahmakiran, S. Ozkar, M. Kaya, RSC Adv. 4 (2014) 28947.

[14]   K. Mori, K. Yamaguchi, T. Mizugaki, K. Ebitani, K. Kaneda, Chem. Commun. 2001 (5) 461.

[15]   A. Indra, C.S. Gopinath, S. Bhaduri, G.K. Lahiri. Catal. Sci. Tech. 3 (201) 1625.

[16]   Y. Masuyama, K. Yoshikawa, N. Suzuki, K. Hara, A. Fukuoka Tetrahedron Lett. 52 (2011) 6916.

[17]   C. Kibby, W.K. Hall, J. Catal. 29 (1973) 144.

[18]   S. Joris, C. Amberg J. Phys. Chem. 75 (1971) 3172.

[19]   S.D. Sebti, R. Tahir, R. Nazih, S.D. Boulaajaj, Appl. Catal. A 218 (2001) 25.

[20]   T. Tsuchida, S. Sakuma, T. Takeguchi, W. Ueda, Ind. Eng. Chem. Res. 45 (2006) 8634.

[21]   A. Solhy, R. Tahir, S. Sebti, R. Skouta, M. Bousmina, M. Zahouily, *et al*. Appl. Catal. A 374 (2010) 189.

[22]   T. Zordan, L.G. Hepler, Chem. Rev. 68 (1968) 737.

[23]   V. Subramanian, H. Zhu, B. Wei, Chem. Phys. Lett. 453 (2008) 242.

[24]   C. Battilocchio, J.M. Hawkins, S.V. Ley Org. Lett. 16 (2014) 1060.

[25]   X. Yu, C. Liu, L. Jiang, Q. Xu Org. Lett. 13 (2011) 6184.

[26]   B. Chen, J. Li, W. Dai, L. Wang, S. Gao Green Chem. 16 (2014) 3328.

[27]   A. Shaabani, M. Borjian Boroujeni, M.S. Laeini Appl. Organomet. Chem. 30 (2016) 154.

[28]   X. Fu, J. Feng, H. Wang, K.M. Ng, Nanotechnology 20 (2009) 375601.

[29]   A. Shaabani, Z. Hezarkhani, S. Shaabani, RSC Adv. 4 (2014) 64419.

[30]   S. Chen, J. Zhu, X. Wu, Q. Han, X. Wang, ACS Nano. 4 (2010 2822.

[31]   X. Wang, Y. Li, Chem. Commun. 7 (2002) 764.

[32]   J. Zhu, J. He, ACS Appl. Mater. Interfaces 4 (2012) 1770.

[33]   T. Hakoda, M.A.Z. Chowdhury, A. Shimada, K. Hirota, Plasma Chem. Plasma Process. 29 (2009) 549.

[34]   A. Shaabani, Z. Hezarkhani, E. Badali, RSC Adv. 5 (2015) 61759.

[35]   A. Shaabani, H. Afaridoun, S. Shaabani, Appl. Organomet. Chem. 30 (2016) 772.

[36] A. Shaabani, H. Afaridoun, S. Shaabani, M.K. Nejad, RSC Adv. 6 (2016) 97367.

[37] S. Mohsenian, M.S. Esmaili, B. Shokri, M. Ghorbanalilu, J. Electrostat. 76 (2015) 231.

[38] S. Maruyama, M. Kurihara, T. Ishigaki, K. Watanabe, T. Takizawa, Y. Moriyoshi, Nippon Kag. Kaish. 1 (2002) 27.

[39] Z.H. Cheng, A. Yasukawa, K. Kandori, T. Ishikawa,

J. Chem. Soc., Faraday Trans. 94 (1998) 1501.

[40] Y. Zhang, C. Zhang, G. Huang, B. Xing, Y. Duan, Electrochim. Acta. 166 (2015) 107.

[41] C.-J. Liao, F.-H. Lin, K.-S. Chen, J.-S. Sun, Biomaterials 20 (1999) 1807.

[42] C. Keresszegi, D. Ferri, T. Mallat, A. Baiker, J. Catal. 234 (2005) 64.